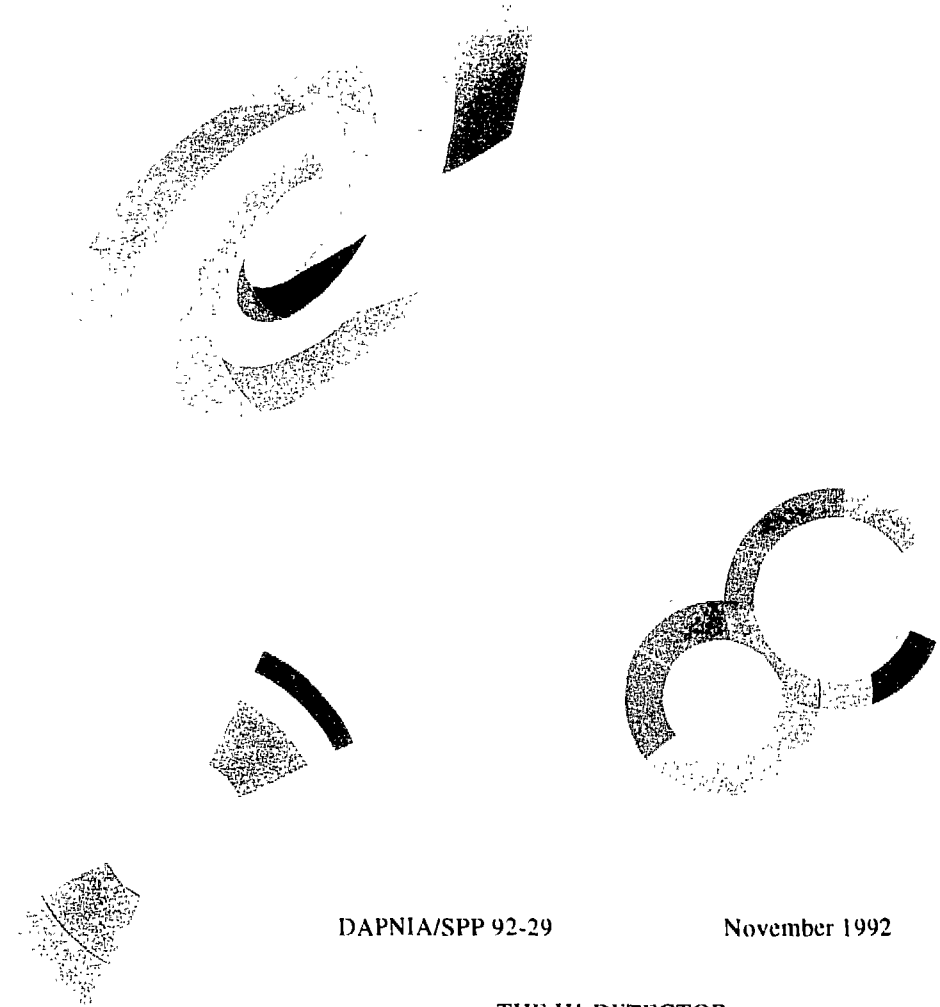


129 2341



SERVICE DE PHYSIQUE DES PARTICULES



DAPNIA/SPP 92-29

November 1992

THE HI DETECTOR

G. COZZIKA

DAPNIA

Contribution to the 3d International Conference on
Calorimetry in High Energy Physics.
September 29 - October 2, 1992, Corpus Christi, Texas

Le DAPNIA (Département d'Astrophysique, de physique des Particules, de physique Nucléaire et de l'Instrumentation Associée) regroupe les activités du Service d'Astrophysique (SAp), du Département de Physique des Particules Elementaires (DPhPE) et du Département de Physique Nucléaire (DPhN).

Adresse : DAPNIA, Bâtiment 141
CEA Saclay
F - 91191 Gif-sur-Yvette Cedex

THE H1 DETECTOR

G. COZZIKA
DAPNIA-SPP, C.E. Saclay
91191 Gif-sur-Yvette, France
H1 Collaboration

ABSTRACT

The H1 detector presently operating at the HERA e-p collider is described. A general overview of the detector is given with particular emphasis on the calorimeters, the main element of which is a liquid Argon calorimeter enclosed within a large radius solenoid. Calorimetry in the proton direction, close to the beam-pipe is provided by a copper-silicon pad hadronic calorimeter. In the electron direction a lead-scintillator electromagnetic calorimeter closes the solid angle between the rear part of the liquid Argon calorimeter and the beam-pipe. An iron limited streamer tube tail catcher using the return yoke of the solenoid as absorber completes the calorimetry of the detector. The hardware triggers derived from the calorimeters are also described and some performance details of the calorimeters are given.

1. Introduction

The HERA electron-proton collider¹ at DESY, Hamburg was completed during 1991 and delivered first luminosity to the experiments in late spring 1992. This machine is the first storage ring of its kind: 30 GeV electrons and 820 GeV protons collide head on, providing a centre of mass energy of 314 GeV which is equivalent to a 50 TeV electron beam hitting a fixed hydrogen target. A completely new kinematical domain will thus open up, reaching Q^2 values of $4 \cdot 10^4$ GeV², about 100 times higher than in fixed target experiments, as well as very small x values, about 100 times lower than in fixed target experiments. Statistical and systematic errors will limit the accessible (Q^2, x) domain, therefore high luminosity and a good understanding of the detector performance, especially regarding calorimeter calibration, are necessary. Absolute systematic errors of respectively $\pm 1\%$, $\pm 2\%$ and $\pm 1\%$ on the absolute energy calibration of the liquid Argon electromagnetic, the liquid Argon hadronic and the backward electromagnetic calorimeters are aimed for. The main goals of the experimental program are tests of the standard model up to regions of high Q^2 ($\leq 4 \cdot 10^4$ GeV²) as well as searches for new physics such as supersymmetric particles, lepton and quark substructures, new bosons or heavy leptons². Consequently the H1 detector was designed to provide clear identification and precise measurement of electrons, muons and penetrating neutral particles together with very good performance in the measurement of jets with high particle densities. These requirements were best met by a calorimeter inside a large coil to minimize both the amount of dead material in front of the electromagnetic calorimeter and the overall size and weight of the calorimeter³. The main reasons for choosing the liquid Argon technique were good stability and ease of calibration, fine

granularity for e/π separation and energy flow measurements as well as homogeneity of response. In addition to good calorimeter resolution and hermiticity, a good identification of electrons and measurement of jets relies on a powerful tracking system. The H1 tracking detector is designed to provide a momentum resolution $\sigma_{p\perp}/p_{\perp}^2$ of $3 \cdot 10^{-3} \text{GeV}^{-1}$ over most of the angular range. First physics results have been presented elsewhere⁴; in this talk an overview of the main elements of the H1 detector including trigger and data acquisition aspects is given but the main emphasis will be on the H1 liquid Argon calorimeter with a short description of each of the following calorimetric components: backward electromagnetic calorimeter (BEMC), forward plug calorimeter (PLUG) and analog tail-catcher (TC).

2. Overview of the H1 Detector

The general structure of the detector⁵ is shown in fig.1. The event topology

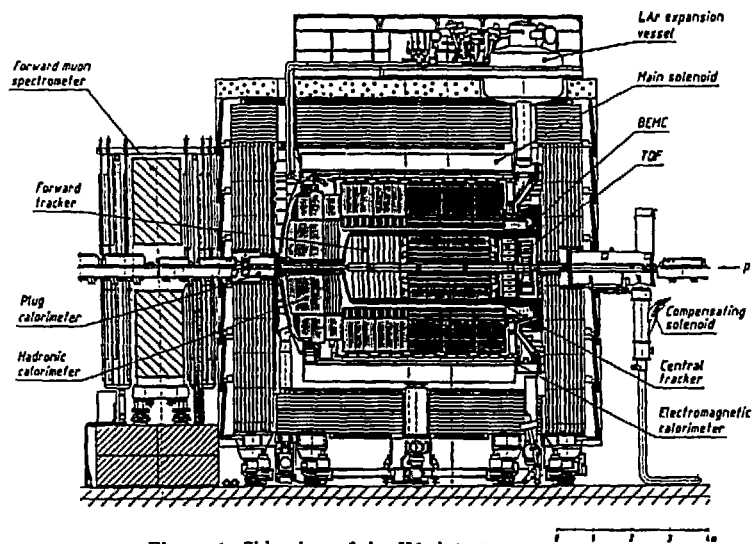


Figure 1: Side view of the H1 detector

of HERA collisions necessarily leads to an asymmetric detector design as the centre of mass of the collision moves fast along the proton direction. Therefore the tracking area is subdivided into two regions: the forward one ($5^\circ < \Theta < 25^\circ$) and the central one ($25^\circ < \Theta < 160^\circ$). A hadronic calorimeter of at least 6λ is needed in the forward (proton) direction whereas in the backward (electron) direction the energy measurement of particles scattered under small angles is provided by the backward electromagnetic calorimeter (BEMC).

2.1. The magnet system

The 1.2T magnetic field is provided by a superconducting solenoid of 2.75 m winding radius within a stainless steel cryostat. This solenoid has a coil geometry similar to the DELPHI magnet, with an overall length of 5.16m. The cryostat

is independent of the liquid Argon cryostat, mainly for logistics reasons at the time of construction. The total radial thickness of the magnet with its cryostat is 0.44m and in average amounts to about 4 r.l. at 90°. Cooling is provided by the main HERA liquid helium supply. The iron structure around the superconducting solenoid serves as a flux return for the magnetic field as well as providing the absorber material for the tail catcher calorimetry and the muon identification. It is divided into three parts, each having its rolling system: the base plate, which carries the solenoid, the liquid Argon calorimeter and the tracking devices, and the two half barrel structures with their end plates. The iron structure has gaps and holes for accomodating cables, cryogenic lines for the solenoid and the liquid Argon system, as well as vacuum pipes for pumping the insulating vacuum in each of the two cryostats. The maximum variation of the field over the sensitive volume of the tracking devices is $\pm 3\%$ so that all second order field dependent corrections for the conversion of drift time into space coordinates are small. To ensure that the field integral along the beam axis is ≈ 0 , a compensating magnet is installed in the rear endcap, downstream of the electron beam. It has a maximum field value of 6T.

2.2. Tracking detector

The tracking detector^{3,6} consists of the central tracker to which is fixed the forward tracker in the proton direction and the backward MWPC in the electron direction. A side view of it, seen mounted on the inner warm vessel of the liquid Argon cryostat, is shown in fig.2. The central tracking detector consists of six sets

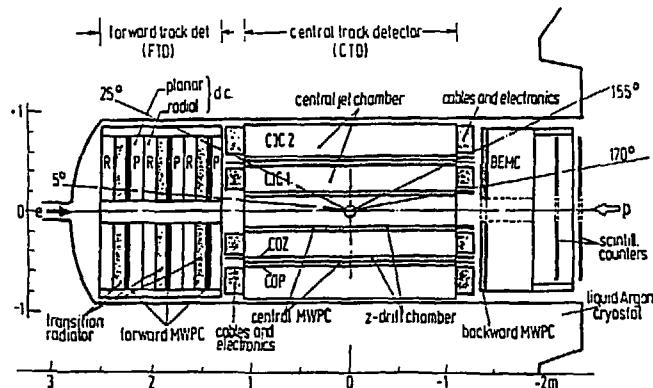


Figure 2: Side view of the H1 tracking system

of cylindrical chambers with independent gas volumes and separate electrostatic shielding. Starting from the interaction vertex a particle is detected by the inner MWPC (CIP)⁷, the inner z-chamber (CIZ)⁸, the inner jet chamber (CJC1)⁹, the outer z-chamber (COZ)¹⁰, the outer MWPC (COP)¹¹ and the outer jet chamber (CJC2)⁹. The CJC1 and CJC2 chambers are based on the jet chambers of JADE and OPAL and use presently, for safety reasons, the gas mixture 89.5% Ar, 9.5% CO₂ and 1% CH₄. The momentum resolution achieved with this gas mixture is $\sigma_{p_T}/p_T^2 \approx 10^{-2} \text{GeV}^{-1}$, the design value of $3 \cdot 10^{-3} \text{GeV}^{-1}$ being reached once the final gas mixture (50% Ar, 50% C₂H₆) is used. In addition these jet chambers have

a hit resolution in the r - ϕ plane of $\sigma_{r\phi} \simeq 160\mu$, provide a z coordinate via charge division ($\sigma_z \simeq 2.5\text{cm}$) and determine dE/dx with a resolution of about 10% at present. The CIZ and COZ drift chambers provide a z -resolution of $\sigma_z \simeq 300\mu$ and the MWPC's are used in the trigger logic. The forward tracker is constructed as a set of three identical 'SuperModules'³ each containing one planar module (three planes of parallel staggered wires orientated at 60° relative to each other; spatial resolution $\sigma \simeq 210\mu$) followed by a MWPC plane, a transition radiator and a radial module¹² (48 angular segments each with 12 sense wires; spatial resolution $\sigma \simeq 210\mu$ and radial coordinate resolution by charge division $\sigma \simeq 2.9\text{cm}$). Interleaving the planar and radial chambers was done to optimize pattern recognition. The MWPCs are used in the forward ray trigger. The tracker system is completed in the backward direction by a MWPC positioned in front of the backward electromagnetic calorimeter. This chamber consists of 4 planar wire planes, the direction of the wires in each plane being rotated by 45° with respect to the neighbouring one. It provides an additional space point for small angle tracks in the central tracker pointing to the BEMC. All drift chambers are equipped with a fast FADC readout and a digital wrap around memory acting as pipeline. The sampling frequency is 104 MHz, ten times the bunch crossing frequency of HERA to ensure precise digitisation.

2.3. Calorimeters

Both electromagnetic and hadronic calorimeters are as hermetic and homogeneous as possible for jet and missing transverse energy measurements. Further requirements for the electromagnetic calorimeter are:

- resolution for electrons: $\sigma(E)/E = 0.10/\sqrt{E}$
- stability of response at the 1% level
- in order to get precise angular reconstruction and to ensure a good e/π rejection ($\leq 10^{-3}$) the readout structure must have a fine transverse and longitudinal segmentation (the lateral dimensions of the pads should be of the order of the Moliere radius) and there should be at least 3 longitudinal segments everywhere.
- the e.m. showers should be fully contained

and for the hadronic calorimeter:

- resolution for hadrons: $\sigma(E)/E \leq 0.55/\sqrt{E}$
- overall stability $\leq 2\%$
- the high energy hadronic showers have to be fully contained when the tail catcher is included.

Thus dead materials and cracks had to be reduced to a minimum and a single cryostat was necessary. Access to the central tracker required a free space for $\Theta \geq 150^\circ$ which is covered by the BEMC. Sections 3 and 4 contain a description of the liquid

Argon calorimeter and the BEMC respectively. A description of the liquid Argon system and some performance results are given in a forthcoming publication¹³.

2.4. Muon detector

The muon detector consists of the instrumented iron covering most of the detector and of the forward muon spectrometer.

2.4.1 Instrumented iron

The return yoke for the magnetic flux is fully instrumented to measure the hadronic energy leaking out of the calorimeters (TC) and to identify and measure muons^{3,14}. It is longitudinally divided into 10 slabs of 7.5 cm thick iron and between each slab are sets of single layer limited streamer tubes (LST) with wire and pad readout. In addition, the muon detection is done by two sets of chambers, one made of two layers of LST's and located between the solenoid and the yoke and the other made of three layers and mounted on the outer part of the yoke. These LST's have wire and strip readout. For safety reasons the LST profiles are made of Luranyl with a low resistivity ($\approx 10 \text{ K}\Omega/\square$) coating painted on, and use a non flammable gas mixture (88.5% CO_2 , 9.5% Isobutane and 2.5% Ar). This mixture proved to be a reliable alternative to the standard 75% Isobutane and 25% Argon mixture. The high voltage working point is lower by $\approx 200\text{V}$ but results from tests-beam measurements at CERN showed that charge spectra and efficiencies for muons were comparable and measurements of hadronic showers showed no significant difference concerning linearity and resolution. However the plateau width is significantly reduced leading to rather delicate operation conditions with respect to temperature and pressure: the high voltage control system monitors the atmospheric pressure and sets the high voltage accordingly. The wires and strips yield spatial information and have their own readout chain. A muon trigger logic¹⁴ provides muon related signals contributing to the first level central trigger. The analog signals from the pads are summed into towers and after amplification, shaping and multiplexing are readout through the liquid Argon chain. Energy resolution of the TC is $\sigma(E)/E \approx 100\%/\sqrt{E}$ as determined from measurements in a CERN test beam. The whole detector consists of about 4000 m^2 of LST planes, 103700 wires, 28700 strips and 4000 pads, the latter being part of the TC system. Presently the detector is about 3/4 equipped, completion being due during the 92/93 winter shutdown.

2.4.2 Forward muon spectrometer

In the forward direction ($3^\circ \leq \Theta \leq 17^\circ$) the muon momentum is measured by a spectrometer consisting of a toroidal magnet with 4 sets of paired drift chambers measuring the polar angle Θ and 2 sets of paired drift chambers measuring the azimuthal angle ϕ . The spatial resolution of these chambers was measured using beam halo muons: $\sigma \leq 350 \mu$. The momentum resolution σ_p/p varies between 25% at 25 GeV/c and 32% at 150 GeV/c.

2.5. Plug calorimeter

The plug calorimeter is in the very forward part of the detector and closes the solid angle between the forward liquid Argon calorimeter and the beam pipe. It is placed behind a large amount of dead material from the cryostat and the beam-pipe. It sees essentially the proton fragments and beam-gas/beam-wall interactions. It

consists of 8 75mm copper plates with silicon pad readout within the gaps, mounted in half disks on the forward end cap of the instrumented iron. This detector will be completed in the course of 1993. Results on the behaviour of the silicon detectors in this high radiation environment are not yet available.

2.6 Luminosity monitor and electron tagger

The luminosity monitor uses $e p \rightarrow e \gamma p$ bremsstrahlung which has a large and precisely calculable cross-section. It consists of a photon detector and an electron tagger set up to measure the γe^- coincidences. The photon detector consists of a hodoscope of 5x5 KRS crystal shower counters of 20x20x200 mm³ and the electron tagger of a hodoscope of 7x7 of the same crystals but of 22x22x200 mm³. Energy resolution is $\sigma/E = 12\%/\sqrt{E} + 1\%$. These detectors are on tables that can be lowered during beam injection to protect the crystals against radiation. Presently, the absolute luminosity value is known to within 7-10 %; further understanding of the acceptance of the system should lower this uncertainty to about 5 %. The electron tagger is also used to trigger on photoproduction events, in which case it is set up with a veto from the photon detector. Other triggers can be setup where the electron tagger is in coincidence with other subdetector triggers of H1.

2.7 Trigger and data acquisition

The HERA bunches are separated by 96 ns; this means that a high rate of beam gas and beam wall triggers will completely saturate the data acquisition system. Therefore a purpose built sophisticated triggering system is used to reject as much as possible of this background ($\approx 10\text{kHz}$) making sure that physics triggers are kept. This first level trigger system¹⁵ uses information from different parts of the detector which are put into a frontend pipeline to delay the trigger decision. The difficulty in this kind of experiment resides in the ability to assign to a given event (i.e. data in the subdetectors) the true bunch crossing t_0 in which this event occurred. Subdetector triggers have to be designed with this 't₀' determination possibility in mind so that coincidences between triggers occurring at the same bunch crossing can be setup thus reducing the trigger rate to more acceptable levels. Fast scintillator counters with a time resolution of the order of the ns, such as the time-of-flight (TOF) counters or the veto-wall system to veto beam halo muons, provide very accurate timing information in this respect. In sect 3.6 the T₀ determination feature of the liquid Argon will be described. Several levels of trigger are needed to reduce the data taking rate to an acceptable level of a few Hz with a dead-time of about 10-20%. Presently there is one hardware fully programmable 'level 1' system with 'trigger bits' consisting of single 'trigger elements' (triggers as supplied by the subdetectors) or combinations of them. There is also one software 'level 4' system¹⁶ processing data from several subdetectors and computing physics quantities such as vertex distributions, track momenta, etc in order to apply cuts and further reject background. Intermediate trigger levels are still in the design stage. The data acquisition chain has been presented elsewhere¹⁷ and is based on bus architectures. On-line reconstruction is done with the full code running in Silicon Graphics machines. The reconstructed data as well as event classification

are available for analyses within a few hours of the data taking.

3. Liquid Argon calorimeter system

3.1 Cryostat and cryogenics

The main requirements for this vessel were to maximize the space available for calorimeters and to keep the wall thickness in front of the electromagnetic calorimeter to a minimum while being able to withstand a maximum pressure of 3 bars and to support the 600t of calorimeter modules and liquid Argon (53 m³). All walls are made of stainless steel except for the inner walls of the warm and cold vessels around the beampipe and the tracker which are made of aluminum alloy. The flat PTFE signal cables for up to 50000 channels are brought out of the cryostat through 24 tubular ports distributed at both ends around the top half of the vessel. Fig.3 shows the principle of such feed-throughs. The temperature gradient between room and liquid Argon temperatures is done within the cables maintained closely packed by the thermal insulator. The latter also fills the space between the wall of the port and the cables thus preventing cold Argon gas to reach the fiber glass block ensuring gas-tightness. These feed-throughs have been extensively tested during the

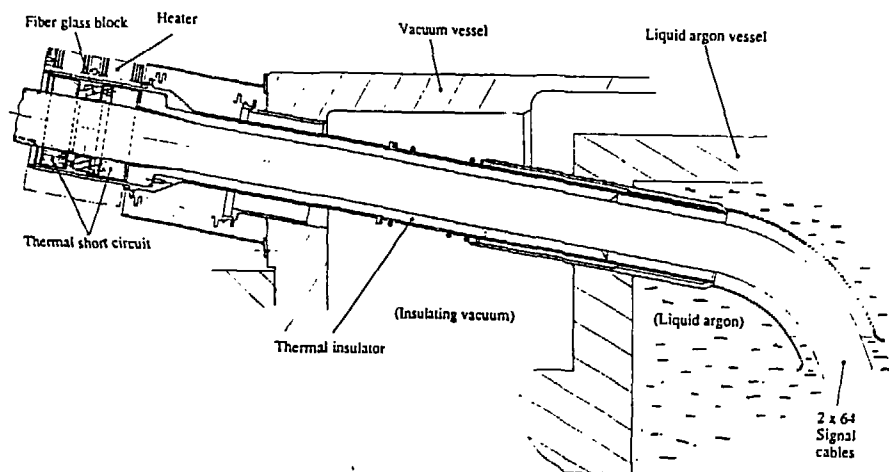


Figure 3: Schematic view of a feed-through for signal cables

various steps of construction and have operated continuously without any problem since early Jan 1991 when the calorimeter was cooled down.

The main design criteria for the cryogenic system were:

- maximum cool-down and warm-up time of 30 days
- transfer of the liquid Argon into the already cold cryostat within 24 hours
- pumping out of the liquid Argon into the storage tank in 2 hours
- to ensure stable temperature and pressure within the cold vessel over several months.

Cooling down to liquid Argon temperature was achieved by circulation of helium gas cooled in an external heat exchanger; the latter was no longer needed once liquid Argon temperature had been reached and was removed. The liquid Argon load (about 53 m³) was transferred from the ground level 70 m³ storage tank into the cryostat through the bottom of the cold vessel. Stable temperature and pressure (1.35 bar) are ensured by a regulated flow of liquid nitrogen through sets of coils located within the cold and the expansion vessels. An Argon purification system is built in but not used presently because of the low level of pollution. Complete control of all processes, including cooldown/warmup and filling/emptying is done by a system of VME automates. Since operations started in early 1991 the calorimeter has remained full of liquid Argon except for a few days in spring 1991 when it was partially emptied to test the emptying procedure and for two weeks in jan. 1992 when the liquid Argon had to be removed to roll the detector into the beam. The average liquid nitrogen consumption was 600 l/h during the cool-down phase and \approx 95 l/h during stable operation. 250 m³ of helium gas and 190 m³ of liquid nitrogen were needed for the 25 days cooldown process.

3.2 Liquid Argon purity monitoring

A liquid Argon purity monitoring system¹³ has been integrated into the H1 calorimeter to check the stability of the ratio *energy loss/ collected charge* at the required level of \ll 1%. The basic sensor is a liquid Argon ionisation chamber to which the nominal electric field (1 KV/mm) is applied. Its cathode is coated with a ²⁰⁷Bi source of 2000 Bq activity. The energy spectrum of the radioactive decays is accumulated and an on-line shape analysis yields the average pulse height corresponding either to the 481 keV conversion-electron peak, or to the upper edge of the spectrum, around 1005 keV. The latter method is more precise (\approx 0.3 %) because it does not suffer from Compton background. There are 11 such probes distributed around the cryostat and their locations are shown in fig.4. Fig.5 shows the relative variation of the charge collected for three of the probes since the cryostat was first filled. Since this date the same load of liquid Argon has been used and the purity measurements show that the signal attenuation is less than 0.5% per year. The break in the curves in January 1992 correspond to the time when the detector was moved into the beam and the liquid Argon had to be pumped out. Furthermore a small movable cryostat is used to measure the quality of liquid Argon at delivery or to cross-checking with the H1 test setup in a CERN test beam.

3.3 Calorimeter modules

The segmentation of the calorimeter followed the basic two-fold requirement of minimizing the dead volumes and of dealing with objects practical to build and handle. Fig.6 shows the segmentation along the beam axis in 8 self supporting 'wheels'. Each of the barrel wheels is segmented in ϕ into 8 identical 'stacks' with pointing cracks in the electromagnetic section and strongly nonpointing cracks in the hadronic section. The 2 forward wheels are somewhat similar in the principle but mechanically are each assembled as two half rings. The ϕ segmentation of the CB wheels is shown in the lower part of fig.6. The hadronic stacks are made of welded stainless steel absorber plates with independent read-out cells inserted between the plates and define the rigid structure on to which are mounted the corresponding electromagnetic stacks. The orientation of the absorber plates is such that particles

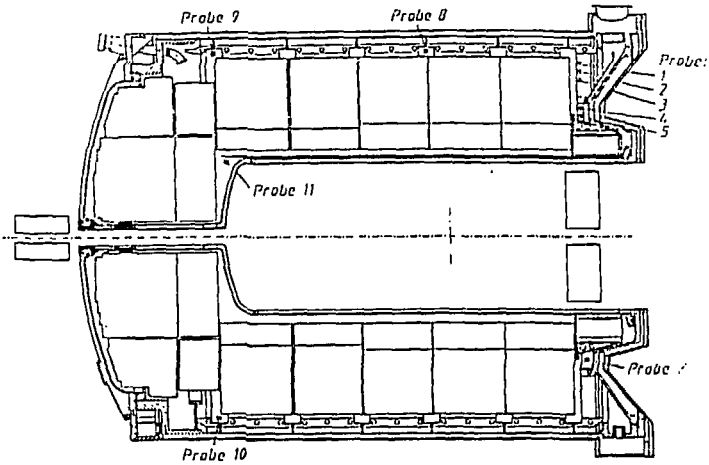


Figure 4: Location of the liquid Argon purity probes within the cryostat

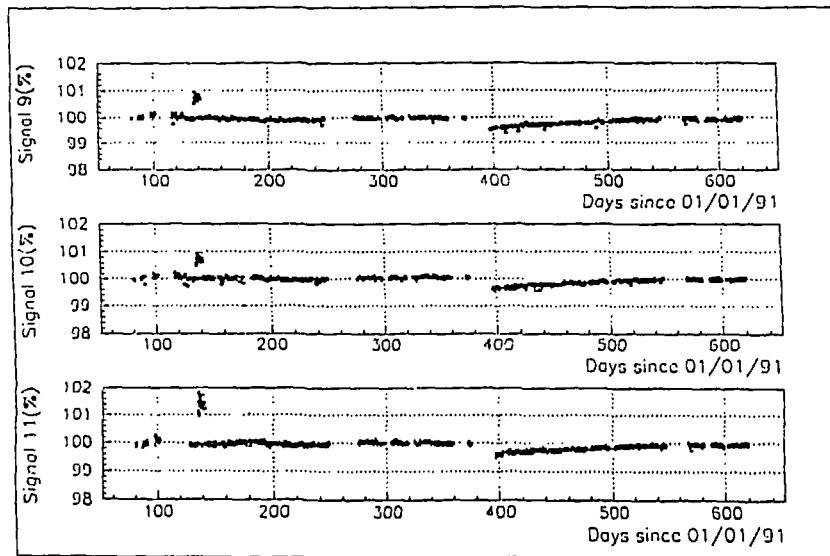


Figure 5: Relative variation of the charge collected for 3 of the probes as a function of time (days since 1/1/1991)

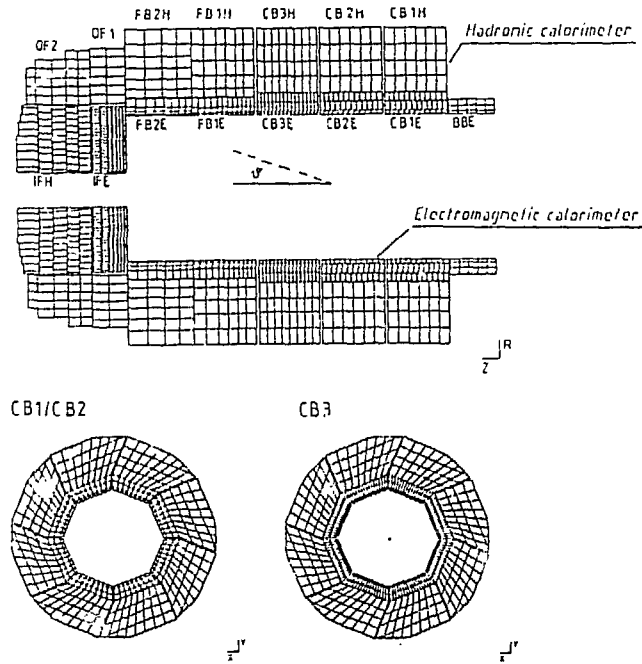


Figure 6: Top: segmentation along beam axis; bottom: ϕ segmentation of CB3 and CB1/CB2 wheels

are incident to the calorimeter with angles not smaller than 45° . The basic structure of each electromagnetic stack consists in a pile of G10-Pb-G10 sandwiches separated by spacers defining the liquid Argon gaps, the basic sampling cell being 2.4mm Pb and 2.35mm liquid Argon with, per gap, one readout plane with pads and one high voltage plane coated with high resistive paint. The hadronic sampling cells consist of a total of 19mm stainless steel, (16mm absorber from the welded structure and 2x1.5mm from the plates of the readout cells defining the active liquid Argon gap) and of a double gap of 2x2.3mm liquid Argon having a G10 board with pads on both sides in the middle of the active gap to collect the charges deposited in the gaps. A kapton foil is glued to the inner side of the stainless steel plates and is coated by a layer of high resistive paint (IF1,FBH,OF stacks) or with copper (CBH). The high voltage is applied to this layer, the kapton providing the decoupling capacity necessary to keep negative crosstalk low and the high resistive coating providing protection against high voltage break-downs. In the case of the copper high voltage plane neon spark gaps are added close to the stacks as active protection. More details can be found elsewhere^{8,13}. The total thickness of the calorimeter varies between 20 and 30 X_0 . Because of the absorber materials and active medium used, this calorimeter is not compensating (the response to electrons is different from that of hadrons); the required resolution is obtained by a software weighting method^{18,19} making use of the large differences in the development of the two components (π^0 's and charged hadrons) of the hadronic showers. This method requires each tower segment to have a depth of about 1 interaction length (λ_{int}). The lines of constant

λ and X_0 are shown in fig.7. The granularity of the read-out cells stems from the

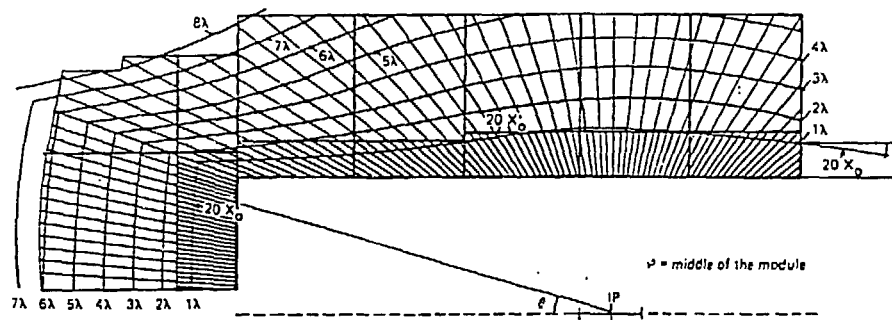


Figure 7: Containment of the liquid Argon calorimeter: iso- X_0 and iso- λ lines

requirements of a good separation of electromagnetic and of hadronic showers and 3 to 4-fold sampling of the longitudinal development of the shower. In addition the overall capacities per channel are below 14nF so that the electronic noise is kept at a reasonable level; An important constraint in the tower size is directly related to the calorimeter trigger, for which the collected energies must belong to a unique bunch crossing t_0 of the accelerator. As this trigger is built from sums of neighbouring tower segments (16 in e.m. and 4 in hadronic) these should have equal capacities within 10%. Therefore the pad area of read-out cells within a trigger tower should have equal area within the same limit. The high voltage distribution is done by 1504 independent lines and each line feeds a group of non consecutive planes in a stack, interleaved with planes linked to another line to reduce the chances that a complete tower segment be dead in case of high voltage problem in one line. Using a trigger based on cosmic rays the average response in the hadronic layers of the central barrel wheels as a function of the applied high voltage was measured for each of the cosmic ray runs that were done while the detector was being commissioned. Such a curve²⁰ is shown in fig.8 for one of the 3 central barrel wheels that were in the acceptance of the cosmic ray trigger. One stack of each type in the detector has been calibrated in a test beam at CERN and because of the care taken to ensure that all mechanical tolerances were kept to during construction of each of the other stacks, it was possible to use a common calibration constant 'pC to GeV' for all stacks of the same type. The present operating voltage of the whole calorimeter is 1.5kV which corresponds to an electric field of 650 V/mm. This is lower than the standard 1000 V/mm used for such liquid ionization chambers but leads to a much more stable operation as regards the number of problematic high voltage channels drawing high currents. Furthermore because of the very small pollution of the liquid Argon, the correction applied off-line to get the collected charge at infinite high voltage is stable and well known from a fit²¹ to the high voltage curve. Presently 3% of the high voltage lines do not reach the full voltage but provision exists in the off-line reconstruction software to take these into account.

3.4 Electronics and data acquisition

The main constraint in the design of the system is that large energies may

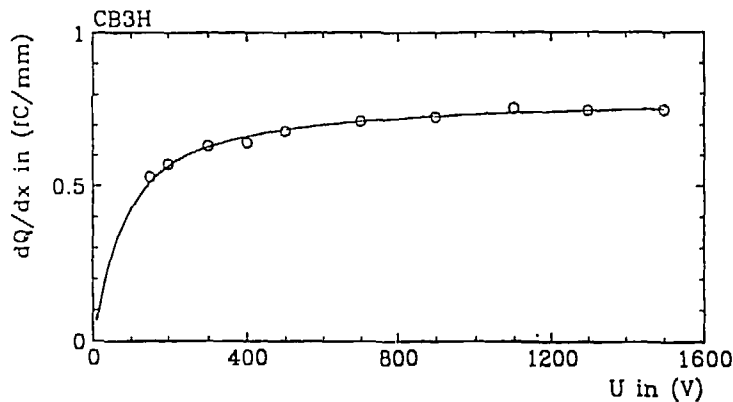


Figure 8: Average response in the hadronic layers of the CB3H wheel as a function of the applied high voltage. Superimposed is a fit using parametrization²¹.

be deposited at short time intervals (96ns at HERA) into detectors with large capacitances and long collection times, and the information has to be stored until the arrival of the trigger signal ($\approx 2.9\mu\text{s}$). Using Monte Carlo simulations to determine maximal signals on one hand and the measured dependence of the electronic noise on the detector capacity ($5500 e_e + 5000 e_e/\text{nF}$ where e_e is the electron charge) on the other hand, the required dynamic range, defined as the ratio of maximal signal to noise, corresponds to 14bits for 25 % of the channels; a 12 bit dynamic range is enough for the remaining 75%. The basic layout of the electronic chain is described elsewhere^{3,13}. The preamplifiers are located just outside of the cryostat and feed on one hand the analog readout system via 2 multiplexers giving an overall 1/128 multiplexing factor, and on the other hand the trigger system which is described in section 3.6. To extend the dynamic range to 14 bits while using a 12-bit ADC, a double transmission with two different gains is used where necessary. The signals are sent twice via $\approx 30\text{m}$ twisted pair lines to differential line receivers located in the analog receiving unit which performs analog baseline subtraction. Each such unit serves 512 calorimeter channels and is connected to an ADC board serving 1024 electronic channels, corresponding to either 512 double gain or to 1024 single gain calorimeter channels. Each ADC board is controlled and readout by a digital signal processor (DSP) module performing basic operations on the data such as pedestal subtraction, zero-suppression and gain correction. This read-out system is described elsewhere^{13,22,23}. The total amount of channels where no signal reaches the preamplifier because of bad contacts within the cryostat is 0.15% and has remained stable over more than a year.

3.5 Electronic calibration

The main goal of this system is to ensure that the calibration of the electronic chain is known and stable to within a few 10^{-3} . The calibration system charges with voltage pulses of very precisely known amplitudes the 47pF calibration capacitors. These have been carefully selected to within $\pm 1\%$. Two systems have been built into the calorimeter: the first one with a high granularity, where the calibration

capacitors are in the liquid Argon for injecting the charge close to the stacks (cold calibration) and the second one with a much coarser granularity in which the calibration charge is injected at the preamplifier level (warm calibration). The first system allows detailed cross-talk studies to be done whereas the second one is used mainly as a backup for calibrating those channels for which some problem has occurred in the calibration line within the cryostat. This is done by using a warm to cold calibration extrapolation method from neighbouring channels and was developed during the runs in test beams at CERN. The hardware consists of 992 pulse generators steered by 4 command modules, each generator pulsing simultaneously up to 64 calorimeter channels. The command module activates selected groups of generators and sets the pulse voltage level by a 16-bit DAC, in the range 0, -1V. The calibration procedure, once the timing of the calibration with respect to the beam particles has been properly set, consists in a high precision determination of the calibration curves (ADC response vs injected charge); this is done each time the current calibration constants are no longer valid because of changes in the hardware or because of pedestal drifts. A third order fit is performed for each channel¹³ from which are determined the constants to be downloaded into the DSP's. At H1 such operations are done once every few weeks, at present, as the stability of the calibration constants over one month is quite good as seen in fig.9. On the short term the hardware and the stability of the electronic chain are monitored regularly.

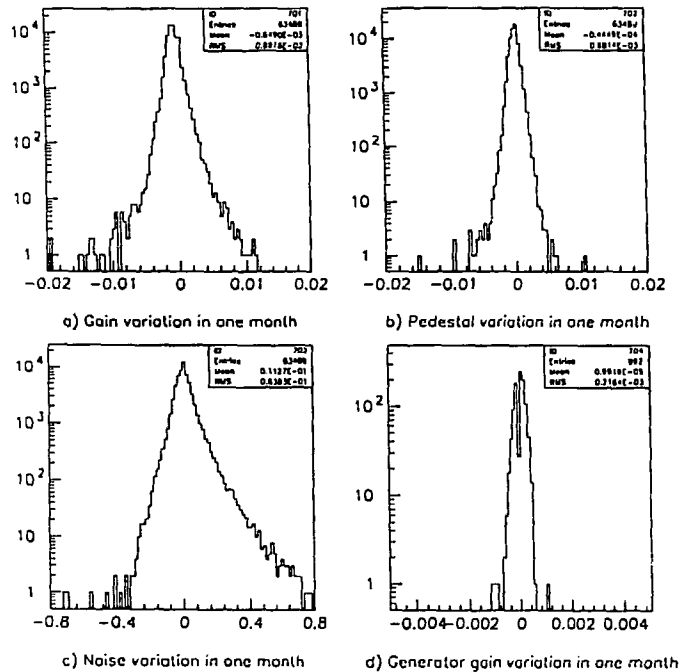


Figure 9: Relative variation of the calibration chain over one month

Pedestal and gain variations are of the order of a few 10^{-3} per month. Noise per channel is about 10-30 MeV depending on the detector capacity.

3.6 Calorimetric triggers

This liquid Argon trigger is an important asset for triggering on high Q^2 events, the study of these being one of the reasons for which HERA was built. An essential constraint in the trigger system for operation in an environment such as HERA is to be able to operate in a correlated way so as to allow combinations of triggers from different subdetectors to be done. One of the main aspects of the triggers described below is the possibility to determine the bunch crossing at which the event triggered upon. Because of its fine granularity the liquid Argon calorimeter is very suitable for providing triggers either in small solid angles or over 4π . The trigger system is divided into an analog and a digital part. The first one combining the 40000 calorimeter channels involved, to provide 256 projective towers (big towers or BT's), divided into electromagnetic and hadronic sections. The second one digitizes the 2×256 BT's with 10MHz ADC's and feeds their signals into digital summing electronics yielding various energy sums (total, barrel, forward, transverse or missing energies). After discrimination by use of programmable threshold functions these sums provide the trigger bits for the central trigger logic. The BT signals are achieved by analog summing of up to 4 trigger towers (TT's). These are sums of longitudinally summed trigger cells which in turn are the sums at the preamplifier box level of a certain amount of pad signals. The TT's are gated by fast analog switches to suppress noise. After digitization, the hadronic and electromagnetic sections are added to form total BT energy sums after relative weighting by look-up tables. These BT sums are used to calculate and discriminate the following quantities:

- topological energies in various parts of the calorimeter
- energy in the barrel part (CB and FB)
- energy in the forward calorimeters (IF + Plug)
- energy in the backward calorimeters (Barrel + BEMC)
- transverse energy
- missing transverse energy
- weighted energy in the calorimeter

The determination of the bunch crossing number of the energy deposition is done in the analog part by means of a pulse delay and crossing technique at the TT level: the crossing point of the original and the delayed TT signal is determined and compared to an amplitude window to exclude noise and saturation effects. The gated t_0 signals are then synchronized with the bunch crossing signal and counted. A number discriminator provides a t_0 signal to the central trigger logic.

3.7 Calorimeter performance

The performance of the liquid Argon calorimeter is reviewed elsewhere at

this conference²⁴. The energy resolution data can be fitted¹³ by the parametrization $\sigma^2/E^2 = (A^2/E) + (B^2/E^2) + C^2$. Results from exposing single stacks to electron beams (3.7 to 80 GeV) at CERN yield from the fit of the energy resolution for electrons $A=(11.16\pm 0.05)\% \cdot \sqrt{GeV}$, $B=152\pm 4$ MeV and $C=(0.64\pm 0.07)\%$. Similarly, using pion beams (3.7 to 170 GeV), the fit to the data yields for the energy resolution for pions $A=(46.1\pm 0.7)\% \cdot \sqrt{GeV}$, $B=730\pm 30$ MeV and $C=(2.6\pm 0.2)\%$. These calibration results show that the resolution requirements given earlier are achieved. With the complete detector data have been taken with cosmic rays over several periods since April 1991. The muon signal is observed to be stable to $\pm 2\%$ between November 1991 and May 1992²⁰. Another method, also using cosmic rays, was to cross-check the momentum measured by the central tracker of low energy electrons generated by muons crossing the detector with the calorimeter response. Agreement is observed at the 2% level at present²⁴. These results show that the overall energy scale for the H1 liquid Argon calorimeter is compatible to that level with the electron beam results. This will improve with better understanding of the detector. Using data taken during HERA operations the hadronic energy scale can be checked but the statistics presently available are a limiting factor. Two methods have been investigated²⁴, the first one being a cross check of the momentum of hadronic charged tracks with the response of the liquid Argon calorimeter. The second one is a p_T balance method involving two independent calorimeters, the BEMC for the electron and the liquid Argon calorimeter for the hadrons. Both methods show that the present data check the hadronic energy scale to about 10%. This should improve significantly with more statistics.

Concerning the trigger, the overall decision time is 21.5 bunch crossings (2.1 μ s). The precision of the t_0 determination is 10ns for a single TT over the full dynamic range and 20ns for the entire system. Trigger thresholds of 2 GeV have been achieved for electrons and 4 GeV for the total energy quantities. However presently, because of not yet understood noise sources, the electron trigger threshold is at 6 GeV and the forward trigger threshold at 15 GeV so as to limit fake electron triggers from background protons. Both barrel and transverse energy trigger low thresholds are now at 6 GeV and the high ones at 13-14 GeV. Further understanding of the noise sources will allow the thresholds to be lowered. Use of the liquid Argon t_0 together with t_0 's from other subdetectors allows a substantial improvement of the trigger sharpness.

During the July 92 run an event with a $Q^2 = 800$ GeV² was observed and is shown in fig.10. The electron is detected in the CB1E calorimeter and several jets can be seen. This event was triggered by the liquid argon electron and barrel triggers.

4. Backward electromagnetic calorimeter

4.1 The BEMC

The backward electromagnetic calorimeter (BEMC) measures the energies of electrons scattered in deep inelastic processes under small angles in the backward direction. A secondary role is the measurement of hadrons from photoproduction and medium or low-x hadronic final states, together with part of the iron tail catcher if hadronic energy leaks out. The detector²⁵ is mounted to the rear of the tracker

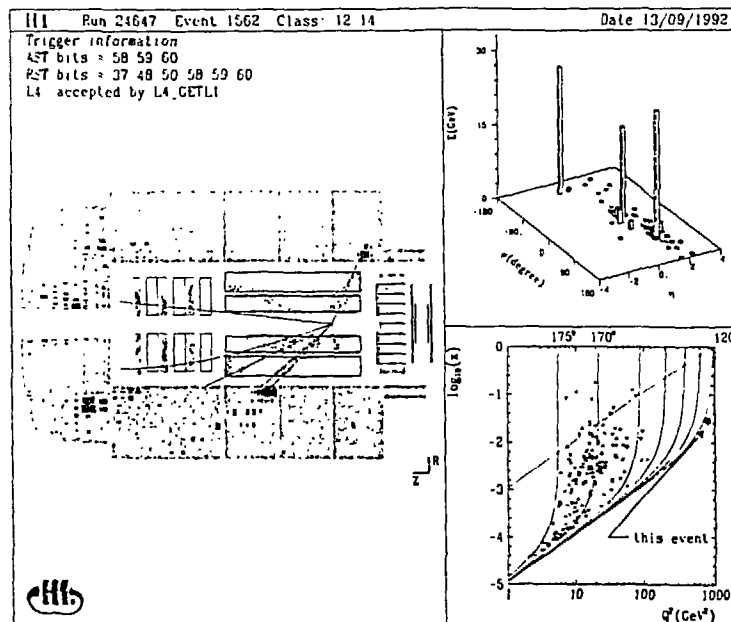


Figure 10: Event with $Q^2 = 800 \text{ GeV}^2$

assembly and covers the polar angular range from 151.4° to 176.5° . Granularity is provided by segmentation into 88 calorimeter stacks parallel to the beam line. These stacks consist of 50 sampling layers of lead-scintillator sandwich amounting to a total sensitive length of $22.5 X_0$, or 0.97λ for the perpendicular impact. One sampling layer consists of 2.5mm lead and 4mm scintillator. Readout is done via wavelengthshifters (WLS) extending over the full length of the stack. In addition the scintillating light produced in the last 6.8 radiation lengths is readout by separate WLS (short). The WLS are connected to Hamamatsu S2575 photodiodes (1 for the long WLS and 2 for the short ones). The electronic chain consists of charge sensitive preamplifiers coupled to the photodiodes and, at the other end of the cables to the electronic trailer, an analog card which gives a unipolar signal faster (FWHM=500ns) than that of the liquid Argon system, for trigger reasons. The rest of the chain, as well as the calibration pulsing system, is identical to the liquid Argon chain. The trigger part is described in section 4.2. The stability of the pedestals and inverse gains was of the order of a few per mille over one month. By performing calibrations weekly the drifts are expected to be kept below the 1 per mille level. BEMC stacks have been measured in test beams at DESY and at CERN. The energy resolution for electrons is $\sigma(E)/E = 10\%/\sqrt{E} + 1\%$. Present work is concentrating on getting the absolute energy scale to the precision of 1%. In deep inelastic events the energy distribution of the electron scattered at small angles should peak at beam energy. This 'kinematical peak' should allow, with enough statistics, to precisely determine the BEMC energy calibration. Present data (till the end of July 92)

show that this calibration is correct at the 3-5% level. To improve the measurement of electrons and hadrons in this area especially to explore the low-x regime of the nucleon structure an upgrade programme is underway with a replacement of the BEMC by a finer granularity calorimeter, either of the SPACAL type or PbF_2 crystals. This will improve the overlap with the liquid Argon calorimeter and extend the calorimeter acceptance closer to the beam line. The backward MWPC will be replaced by a silicon tracker and a drift chamber which will provide a precise measurement of the impact point in front of the backward calorimeter as well as track elements over the full angular coverage of the calorimeter.

4.2 Backward single electron trigger

The backward part of the H1 detector is exposed to a high background. Rates from beam-wall and beam gas interactions are of the order of tens of kHz whereas the rate of deep inelastic events is about 5 orders of magnitude smaller. Discriminating power against background events is therefore essential. The basic idea of the backward single electron trigger²⁶ is to look for well localized high energy depositions in BEMC stacks or groups of stacks called clusters. This purpose made pipelined trigger provides first level trigger signals with certain conditions on the cluster energies, as well as timing information: the history around the nominal trigger can be recorded via a digital pipeline.

5. Conclusion

The H1 detector has been in operation for already more than 18 months and the calorimeters have been operational throughout this period with very few problems. Significant are the stability results on the few per mille level over several months for the purity of the liquid Argon and the electronic calibration. First performance results indicate that the design goals will be achieved. Experience needs to be gained with the liquid Argon trigger which is a powerful tool, together with other triggers in the experiment, to enable the new kinematical domain opened by HERA to be probed.

6. Acknowledgements

I would like to acknowledge the hard work of all the technicians, engineers and physicists who have contributed to develop the H1 detector from a paper sketch to its present state. Special thanks to my H1 colleagues who helped me in the preparation of this talk by supplying useful information and advice.

7. References

1. R. Brinkmann, *The status of HERA*, these Proceedings.
2. *Proceedings of the Workshop 'Physics at HERA'*, Vol.1-2, DESY, October 1991
3. *The Technical Proposal for the H1 Detector*, DESY, March 1986.
4. F. Eisele, *First results from H1 at HERA*, Proceedings of the 1992 Dallas High Energy Physics Conference.

5. F. Brasse, *The H1 Detector at HERA*, Proceedings of the 1992 Dallas High Energy Physics Conference.
6. J. Bürger, *Tracking at H1 in the environment of HERA*, Proceedings of the 4th San Miniato Topical Seminar on Experimental Apparatus..., San Miniato, 1990, p272-283.
7. K. Müller et al., NIM, A312 (1992) 457-466.
8. S. Egli et al., NIM, A283 (1989) 487-491.
9. J. Bürger et al., NIM, A279 (1989) 217-222.
10. U. Bärwolff et al., *A cylindrical Z-Drift chamber for H1*, Proceedings of the 4th San Miniato Topical Seminar on Experimental Apparatus..., San Miniato, 1990, p284-293.
11. G. Bertrand-Coremans et al., Nucl. Phys. B16 (1990) 518-519.
12. G.A. Beck et al., NIM, A283 (1989) 471-476.
13. H1 Calorimeter Group, *The H1 Liquid Argon Calorimeter System*, to be submitted to NIM.
14. J. Tutas, *The Limited Streamer Tube System of H1*, Proceedings of the 1992 Dallas High Energy Physics Conference.
15. E. Elsen, *The H1 Trigger and Data Acquisition System*, Int. Symp. on Electronic Instrumentation in Physics, Dubna, May 1991.
16. A.J. Campbell, *A RISC Multiprocessor Event Trigger for the Data Acquisition of the H1 Experiment at HERA* IEEE Transactions on Nucl. Sci., Issue 2, p255-258.
17. W.J. Haynes, *Bus based Architectures in the H1 Data Acquisition System*, Int. Conf. on Open Bus Systems 92, Zurich, Oct. 1992.
18. H. Greif, PhD Thesis, Munich 1990.
19. H1 Calorimeter group, *Study of Software Compensation for Single Particles and Jets in the H1 Calorimeter*, Contrib. pap. to the XXV Int. Conf. on High Energy Physics, Singapore 1990.
20. J. Stier, *Kalibration des H1 Flüssig-Argon Kalorimeters mit Kosmischen Myonen*, Diplomarbeit Univ. Hamburg, 1992.
21. W. Hofmann et al., NIM, A135 (1976) 151.
22. F.M. Descamps, *The Data Acquisition System of the H1 Calorimeters*, these Proceedings.
23. C. Vallée, *DSP's and AMD 29000 in the H1 Calorimeter DAQ*, CHEP 92, Annecy Sept. 1992.
24. J. Gayler, *Performance of the H1 Liquid Argon Calorimeter*, these Proceedings.
25. BEMC group, *The Backward e.m. Calorimeter*, H1 Internal Rep. H1-08/92-233.
26. BEMC group, *The BEMC Single Electron Trigger*, H1 Internal Rep. H1-07/92-235.